Cerebral Cortex, March 2020;30: 1318–1329

doi: 10.1093/cercor/bhz168
Advance Access Publication Date: 9 August 2019
Original Article

ORIGINAL ARTICLE

N-cadherin (Cdh2) Maintains Migration and Postmitotic Survival of Cortical Interneuron Precursors in a Cell-Type-Specific Manner

Zsófia I. László[1,3,†], Kinga Bercsényi[2,4,†], Mátyás Mayer[2], Kornél Lefkovics[2], Gábor Szabó[2], István Katona[1] and Zsolt Lele[1,2,‡]

[1]Momentum Laboratory of Molecular Neurobiology, Institute of Experimental Medicine, Hungarian Academy of Sciences, Budapest, Hungary [2]Laboratory of Molecular Biology and Genetics, Institute of Experimental Medicine, Hungarian Academy of Sciences, Budapest, Hungary [3]Szentágothai János Doctoral School of Neuroscience, Semmelweis University, Budapest, Hungary [4]Current address: Centre for Developmental Neurobiology, Institute of Psychiatry, Psychology and Neuroscience, and Medical Research Council Centre for Neurodevelopmental Disorders, King's College London, London, UK

Address correspondence to Zsolt Lele, IEM HAS, Szigony utca 43, Budapest, H-1083, Hungary. Email: lele.zsolt@koki.mta.hu.
http://orcid.org/0000-0003-2672-144X
† Shared first authors

Abstract

The multiplex role of cadherin-based adhesion complexes during development of pallial excitatory neurons has been thoroughly characterized. In contrast, much less is known about their function during interneuron development. Here, we report that conditional removal of N-cadherin (Cdh2) from postmitotic neuroblasts of the subpallium results in a decreased number of Gad65-GFP-positive interneurons in the adult cortex. We also found that interneuron precursor migration into the pallium was already delayed at E14. Using immunohistochemistry and TUNEL assay in the embryonic subpallium, we excluded decreased mitosis and elevated cell death as possible sources of this defect. Moreover, by analyzing the interneuron composition of the adult somatosensory cortex, we uncovered an unexpected interneuron-type-specific defect caused by *Cdh2*-loss. This was not due to a fate-switch between interneuron populations or altered target selection during migration. Instead, potentially due to the migration delay, part of the precursors failed to enter the cortical plate and consequently got eliminated at early postnatal stages. In summary, our results indicate that Cdh2-mediated interactions are necessary for migration and survival during the postmitotic phase of interneuron development. Furthermore, we also propose that unlike in pallial glutamatergic cells, Cdh2 is not universal, rather a cell type-specific factor during this process.

Key words: cell death, interneuron development, N-cadherin, mouse, somatosensory cortex

Introduction

The complex structure of the adult neocortex is a result of parallel and synchronized migratory events that bring the excitatory and inhibitory neurons from their birthplace to the proper layer and area of the cortex (Parnavelas 2000; Kriegstein and Noctor 2004). Future glutamatergic cell precursors are born in

the ventricular zone (VZ) of the pallium and migrate radially to form the cortical layers via a multistep process including a transitional amplifying intermediate progenitor cell stage located in the subventricular zone (SVZ) (Bystron et al. 2008). In contrast, inhibitory neurons of rodents are born in subpallial regions: the medial and caudal ganglionic eminences (MGE, CGE) and the preoptic area (POA) (Ang et al. 2003; Marín and Rubenstein 2003; Ayala et al. 2007; Valiente and Marín 2010). Additionally, a significant percentage of interneurons are produced in the pallium of the primates (Letinic and Rakic 2001; Bystron et al. 2008; Radonjić et al. 2014). The inhibitory neuron precursors then migrate large distances tangentially to find their cortical target area, followed by radial migration in order to settle into their final position in the appropriate cortical layer. Disruption of interneuron development and consequent changes in excitatory–inhibitory balance in the adult cortex is thought to be involved in a wide range of neurological diseases including epilepsy, autism, and schizophrenia; therefore, gaining a better understanding of the cellular and molecular pathways involved is essential (Levitt et al. 2004; Metin et al. 2008; Rubenstein 2011; Marín 2012). While the main mechanisms guiding precursor migration of future excitatory neurons have been investigated in detail, the much more complex regulation of inhibitory neuron precursor guidance is currently less clear. Recently, several large-scale single-cell RNA sequencing studies have revealed the transcriptomic landscape of early events in interneuron development (Mayer et al. 2018; Mi et al. 2018; Tasic et al. 2018). These experiments however only indicate the potential role of various molecules; functional studies are still essential in order to specify the task of each molecule as well as their potential interactions.

Type I classic cadherins form a group of Ca^{2+}-dependent and intracellularly β-catenin-binding homophilic adhesion molecules involved in several aspects of neural development (Redies et al. 2000; Takeichi and Abe 2005; Hulpiau and van Roy 2009; Hirano and Takeichi 2012). In particular, plenty of evidence indicates the importance of N-cadherin in maintaining the pallial neural progenitor niche via Akt and Wnt signaling (Zhang et al. 2010, 2013; Rousso et al. 2012). The cadherin-based adherens junction belt prevents migration of the proliferating neuroepithelial and radial glia progenitor cells away from the VZ both in lower (Gänzler-Odenthal and Redies 1998; Lele et al. 2002) and higher order vertebrates (Kadowaki et al. 2007; Franco et al. 2011). In mammals, a reelin-dependent, Dab1/Rap1-mediated N-cadherin expression is also necessary for the final, somal translocation phase of neuroblast migration (Franco et al. 2011; Jossin and Cooper 2011; Gil-Sanz et al. 2013). Consistently, it has been demonstrated that proper regulation of N-cadherin turnover via membrane trafficking is essential for this process (Kawauchi et al. 2010; Linford et al. 2012). In sharp contrast to the wealth of information about the role Cdh2 plays in radial migration of pyramidal cell precursors, it is currently unclear whether it plays a similar dual role during interneuron development. Recently, the importance of Cdh2 in organizing the MGE proliferative zone and determining directionality and motility of postmitotic neuroblasts was demonstrated, but the long-term fate of interneurons in *Cdh2*−/− mice was not investigated (Luccardini et al. 2013, 2015).

Here, using a conditional loss-of-function model, we demonstrate that Cdh2 has a role in promoting tangential migration of subpallial-derived postmitotic precursor cells. Lack of N-cadherin in postmitotic GABAergic progenitors delays their migration to the cortex. More importantly, by carrying out detailed quantitative analysis of various interneuron types of the adult somatosensory cortex in *Cdh2*−/− animals, we demonstrate that this delay eventually leads to a marked cell-type-specific decrease in the number of calretinin- and somatostatin-positive cortical interneurons. We also present evidence that rules out a decreased mitotic activity or increased early cell death in the subpallium as possible causes. Finally, we demonstrate that improper positioning of some of the precursors in early postnatal stages due to delayed migration leads to their elimination from the SVZ.

Materials and Methods

Animals, Sample Preparation, and Sectioning

Animals were kept according to standard protocols controlled by institutional regulations (License No. XIV-I-001/2332–4/2012), which adhere to the Act of Animal Care issued by the Hungarian Ministry of Economy and Environmental Protection (1998, XXVIII, Section 243/1998, renewed in 40/2013) based on appropriate EU regulations (86/609/EEC; Section 243/1998). Crosses of dlx5/6-Cre (kind gift of J. Rubenstein, UCSF) and $Cdh2^{fl/fl}$ (from Jaxmice strain #07611) were made then crossed to Gad65-GFP mice (López-Bendito et al. 2004). +/+ and −/− in the paper refers to *Dlx5/6i-Cre*$^{+/+}$; *Ncad*$^{fl/fl}$ and *Dlx5/6i-Cre*$^{Cre/+}$; *Ncad*$^{fl/fl}$ animals, respectively.

Adult and adolescent animals were anesthetized with the appropriate dose of 1.25% avertin (2,2,2, −tribromoethanol, Sigma, T48402; 2-methyl-2-butanol, Sigma, 152 463 in water) administered intraperitoneally, perfused transcardially with 4% PFA/PB, and removed brains were postfixed overnight in the same buffer. E14 mouse brains were quickly removed after decapitation and fixed overnight in 4% PFA/PB. Adult brains were sectioned at 40 µm for in situ hybridization and immunohistochemistry on a Leica1000 vibratome (Leica). Sections were collected in 24-well cell culture plates and stored at 4°C in PBS until further use but for a maximum of 2 weeks.

E14 mice were collected, decapitated, and fixed in 4% PFA/PB immediately. The heads were equilibrated in 15% and 30% sucrose/PBS for cryoprotection, embedded in Tissue-TEK OCT compound (Sakura Finetek USA Inc.), and sectioned at 20 µm on a MICROM HM 550 cryostat (Thermo Fisher Scientific). Sections were then pulled onto Superfrost Ultra Plus glass slides (Thermo Fisher Scientific) and stored at −20°C until further use.

Cloning procedures, RNA preparation, RT-PCR

For cloning of the probes used for in situ hybridization, total RNA was isolated from E16 and adult mouse brain using Ambion RNAqueous-4PCR kit (Thermo Fisher Scientific, AM1914) according to the manufacturer's protocol. Reverse transcription was carried out using the Maxima First Strand cDNA Synthesis Kit (Thermo Fisher Scientific, K1672). Fragments were amplified via RT-PCR, using the appropriate primers and then cloned into a pGEMT-Easy vector according to the manufacturer's protocol (Promega). The orientation of the incorporated fragment was checked with restriction analysis. Used primers for cloning: *Vip* 5′-CCTGGCATTCCTGATACTCTTCAG-3′ and 5′-TTCTCTGATTTCAGCTCTGCCCAG-3′; *Sst* 5′-TGAAGGAGACGC TACCGAAGCCG-3′ and 5′-TGCAGGGTCAAGTTGAGC ATCG-3′; *Calb2* 5′-GATGCTGACGGAAATGGGTACATTG-3′ and 5′-CCTACCAGCCAC CCTCTCTCCATC-3′; *Npy* 5′-AGAGGCACCCAGAG CAGAG-3′ and 5′-AATGGGGCGG AGTCCAGCCTAGTG; *Cnr1*

5′-ATGAAGTCGATCTTAGACGGCCTTG-3′ and 5′-TCACAGAGCC TCGGCAGACGTGTCTG-3′; *Reln* 5′-TCGCACCTTGCTGAAATACAC AGTG-3′ and 5′-GCCGCATCCCAAATTAATAGAAAAC-3′.

In vitro transcription and in situ hybridization.

In vitro transcription and in situ hybridizations were carried out on 40-µm thick vibratome sections as described previously (Mayer et al. 2010). Essentially, template DNA was created by linearizing the plasmid at the 5′ end of the insert with the proper enzyme, followed by agarose gel electrophoresis and fragment isolation (GeneJET Gel Extraction Kit, Thermo Fisher Scientific, K0691). In vitro transcription was carried out using 2 µg of linear template, DIG-UTP (Roche), and the appropriate RNA polymerase (T3, T7, SP6, Promega). This was followed by RNA purification with RNA Clean & Concentrator kit (Zymo Research, R1013). Before hybridization, sections were rinsed with PBSTw (PBS + 0.1%Tween20) several times. Prehybridization were done using Hyb + buffer (50%formamide, 5xSSC, 0.1%Tween20, 100 µg/ml yeast tRNA, pH:6.00). Hybridization was carried out in the same buffer with the probe overnight at 65°C. Next day, the remaining probe was removed by several rounds of washes using formamide/SSCT, 2xSSCT, and 0.2xSSCT, all at 65°C. After this, sections were transferred to PBSTw then blocked with 2% FBS, 2 mg/ml BSA in PBSTw at room temperature and incubated with the anti-DIG Fab fragment (1:4000 Roche) in the blocking solution at 4°C overnight. Staining was done after extensive washes in PBSTw and TBSTw (0.1 M TrisHCl, pH:9.5, 100 mM NaCl, 50 mM Mg2Cl, 0.1% Tween20) using NBT/BCIP solution (Roche) dissolved in TBSTw. Staining was stopped with PBSTw washes and 4% PFA in PBSTw. Sections were pulled onto Superfrost glass slides (Thermo Fisher Scientific), mounted with Aqua-Poly/Mount (Polysciences Inc.) and sealed with nail polish.

Immunohistochemistry, TUNEL assay

Cryosections were postfixed on the slides using 4%PFA/PB for 15 min, after this step the procedures for cryosections and vibratome sections are almost the same. Sections were washed with PBS several times and permeabilized with 0.2–0.3% TritonX containing PBS to allow better penetration of the antibodies (15′ for cryosections, 30′ for vibratome sections). This was followed by a 1 h long blocking in 5% NDS/PBS (Normal Donkey Serum Sigma A1653) and overnight incubation at 4°C using the following primary antibodies: anti-parvalbumin (Swant, PVG214, 1:3000, goat), anti-phospho-Histone H3 (Millipore, 06–570, 1:500, rabbit), anti-calretinin (Millipore, MAB1568, 1:000 mouse), anti-somatostatin (Santa Cruz, sc-7819, 1:1000, goat). After incubation, sections were washed with PBS and secondary antibodies were applied: Alexa 594 conjugated anti-goat, anti-mouse, or anti-rabbit; Alexa-647 conjugated anti-goat (Jackson Immunoresearch) for 2 h at room temperature.

TUNEL assays were carried out using the ApoptagRed kit (Millipore, S7165) according to the manufacturer's instructions. Immunohistochemistry and TUNEL sections were both mounted using Vectashield Hard Set (Vector Labs H1400) and sealed with nail polish.

Microscopy, image analysis, statistics

Pictures were taken with a Zeiss Axioscope2 equipped with an Axiocam Hrc cooled digital camera or a Nikon Eclipse i80 microscope equipped with a Nikon DsFi CCD camera.

For taking the fluorescent images, Nikon A1R confocal microscope was used. Pictures were always taken using identical settings between +/+ and −/− samples. Cropping, inverting (in case of the in situ hybridization samples), and resizing of the images were done using Adobe Photoshop CS5. Minor contrast enhancement to eliminate background were also carried out when necessary, in these cases, all +/+ and −/− images were treated with identical settings of level correction. To quantify the cell number from the in situ hybridization experiment, GFP-signals, TUNEL-, and immunostainings, images were converted to black and white. Cell density was measured by ImageJ cell counter plug-in, which have been adjusted for each probe used but were always identical between +/+ and −/− samples. Finally, values were normalized to the size of the ROI (cell density). To investigate the distribution of GFP- and TUNEL-positive cells in the cortex, X,Y coordinates were given to each cell, then Y values were differentiated in 10 equal bins and percentage occurrence was counted for each bin. Interneuron migration assay was performed by counting manually the GFP-positive cells in the pallium from the pallial–subpallial boundary.

Statistical analysis of the raw data was done with the Graphpad Prism 5.0 (Graphpad Inc., La Jolla, CA). All experiments were replicated on at least 3 different animals. Kolmogorov–Smirnoff or Shapiro–Wilk tests were used for determining Gaussian versus non-Gaussian distribution of datasets. To determine the poolability of the animal's datasets in each experiment, Kruskal–Wallis test was carried out followed by post hoc Dunn's Multiple Comparison Test. To compare nonpoolable raw data, mean values were tested in a nonparametric manner. In case of normal distribution, 2-tailed unpaired Student's *t*-test was used, while on nonparametric datasets, Mann–Whitney *U* test was applied. Figures show statistical significance with *P*-value and standard classification star system (* means $P < 0.05$, **means $P < 0.01$, and *** means $P < 0.001$).

Results

Dlx5/6i-Cre Eliminates *Cdh2* From the Postmitotic Cells of the Ganglionic Eminences and Delays Embryonic Interneuron Precursor Migration

Cdh2 is expressed very strongly in the ventricular (VZ) and more moderately in the subventricular (SVZ) and postmitotic zones of the ganglionic eminences (SVZ-migratory zone; Fig. 1A). In order to address its importance in tangentially migrating interneuron precursors, we eliminated *Cdh2* in the postmitotic cells of the ganglionic eminences and the POA using a Cre line (Monory et al. 2006) driven by the previously described *Dlx5/6i* regulatory element (Ghanem 2003; Ghanem et al. 2007, 2008). As expected, expression of *Cdh2* (Fig. 1A) was completely missing in the postmitotic area of the ganglionic eminences (marked by a + sign in Fig. 1A,B), while normal expression is maintained in the VZ of the eminences (marked by arrows) and other areas such as the hippocampus (h) or the thalamus (th). Notably, the expression is also missing from the striatal area (str).

In order to find out if lack of N-cadherin in postmitotic migratory cells affects interneuron numbers and/or distribution, we created a triple transgenic line using the Gad65-GFP mouse line (López-Bendito et al. 2004). As a first step, we analyzed the distribution of the Gad65-GFP interneuron precursor population in the E14 cortex. Gad65-GFP marks mainly CGE-derived

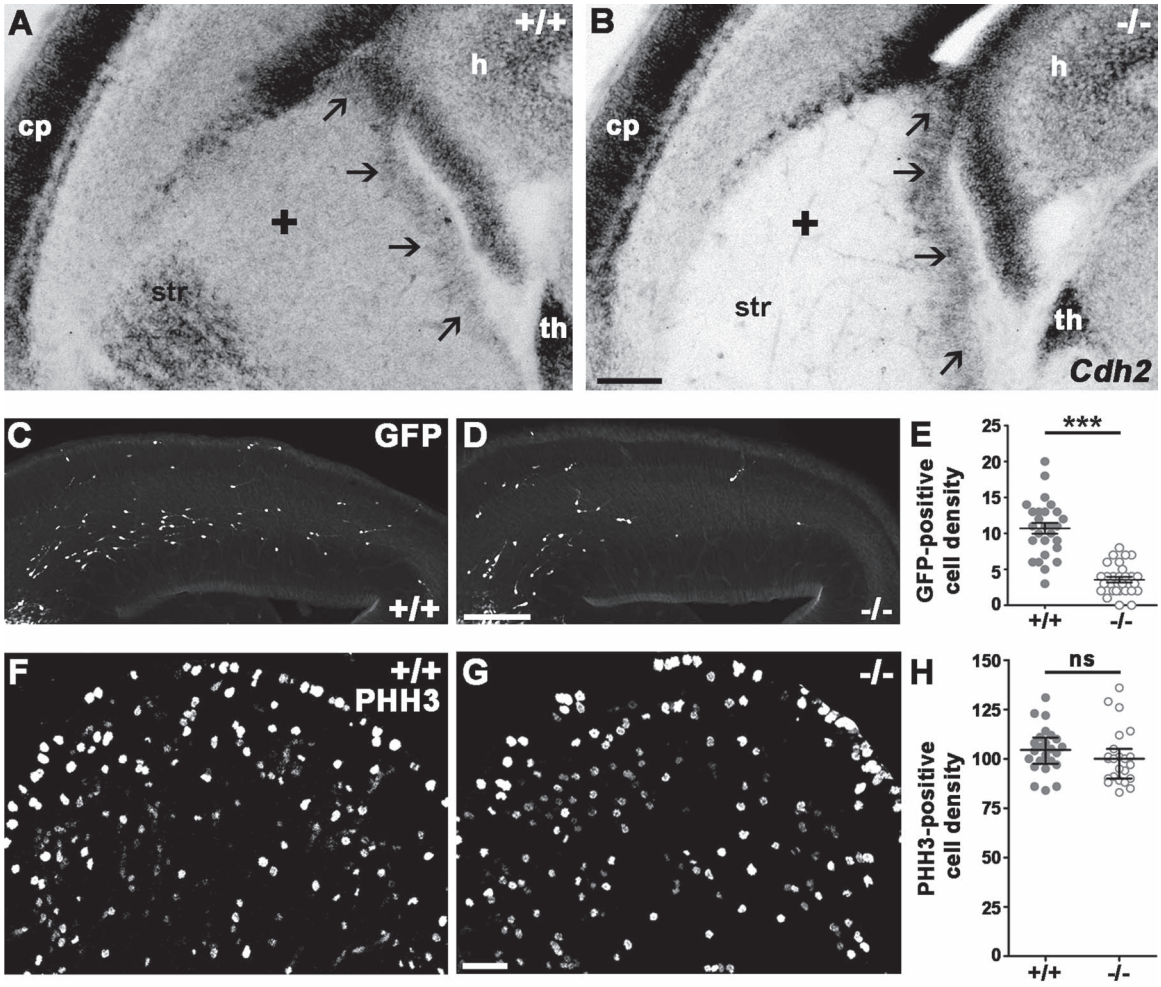

Figure 1. Absence of *Cdh2* from postmitotic interneurons affects the tangential migration but not the proliferation. (*A*, *B*) *Cdh2* mRNA is expressed in the ganglionic eminences of E14.5 +/+ mice (Dlx5/6-Cre$^{+/+}$;Ncad$^{fl/fl}$;Gad65-GFP; black arrows mark the VZ; black + marks the SVZ-migratory zone). Dlx5/6-Cre activity eliminates Cdh2 selectively from the subpallial postmitotic zone and striatum of the −/− (Dlx5/6-Cre$^{Cre/+}$;Ncad$^{fl/fl}$;Gad65-GFP) embryos. Note that similar effect is not detectable in the VZ of the ganglionic eminences, in the thalamus, or in the pallial SVZ. (*C*, *D*) Lack of *Cdh2* causes migration delay of GFP-positive interneurons in −/− E14.5 embryos. (*E*) Statistical analysis shows significantly less GFP-positive interneuron in the pallium of the −/− embryos. Two-tailed unpaired *t*-test, +/+: $n = 3$, 10.7 ± 0.7488; −/−: $n = 3$, 3.552 ± 0.3895; $P < 0.0001$. Graph shows raw data points and means ± SEM. (F–H) Elimination of postmitotic *Cdh2* does not affect the proliferation in the ganglionic eminence of *Cdh2* −/− animals at E13.5. Statistical analysis: 2-tailed Mann–Whitney *U* test, $P = 0.1389$; +/+: $n = 3$; −/−: $n = 3$. Graph shows raw data points and medians ± interquartile range (IQR). *n* indicates the number of mice per group. Scale bars indicate 100 µm (A–D) and 25 µm (F,G); cp: cortical plate, h: hippocampus, th: thalamus, str: striatum.

precursors (López-Bendito et al. 2004). There are already significantly less migrating interneuron precursors entered into the pallium at this stage (Fig. 1C,D,E; +/+: $n = 3$, 10.7 ± 0.7488; −/−: $n = 3$, 3.552 ± 0.3895; $P < 0.0001$) confirming an earlier report (Luccardini et al. 2013) and indicating the necessity of Cdh2 during the precortical stage of interneuron precursor migration.

The decreased number of migrating interneuron precursors in the E14 pallium (Fig. 1C,D,E) could be the result of decreased cell proliferation in the subpallium. Since the *dlx5/6i* promoter driving the Cre is active only in postmitotic cells (Fig. 1A,B), this possibility is unlikely. Nevertheless, we still examined whether Cdh2 loss changes cell proliferation in the ganglionic eminences (Fig. 1F,G) because of its previously proposed role in regulating progenitor proliferation in both the pallium and subpallium (Zhang et al. 2010, 2013; Gil-Sanz et al. 2014; Luccardini et al. 2015). We, however, could not detect a significant difference between the number of mitotic cells (marked by anti-phospho-Histone H3 antibody, PHH3) of +/+ and −/− subpallium (Fig. 1H; +/+: $n = 3$, 104.5 ± 2.336; −/−: $n = 3$, 100.7 ± 2.964; $P = 0.1389$).

Lack of Postmitotic Cdh2 Decreases Interneuron Numbers in the Adult Somatosensory Cortex

To assess the long-term effect of postmitotic Cdh2-loss, we counted Gad65-GFP expressing cells in the adult primer somatosensory cortex of +/+ and −/− animals. This revealed a significant decrease in the number of GFP-positive cells in the knockout cortices (Fig. 2A–C; +/+: $n = 6$, 106.8 ± 2.625; −/−: $n = 6$, 69.44 ± 2.335; $P < 0.0001$). In contrast, analyzing the distribution of the GFP-positive cells within the cortex of +/+ and −/− animals, however, did not reveal any significant difference (data not shown) suggesting that cells are missing equally from all layers of the cortex.

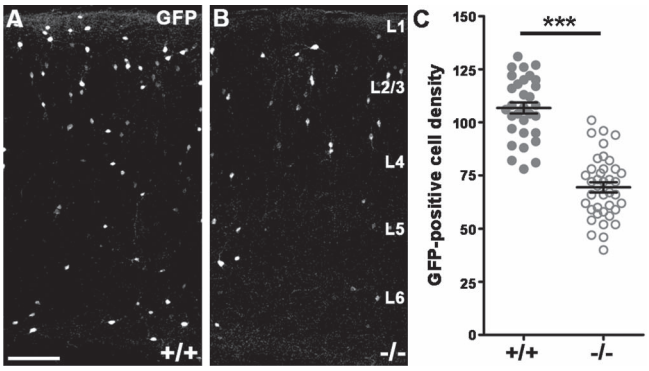

Figure 2. The number of Gad65-GFP-expressing cells falls significantly in the somatosensory cortex of adult −/− animals. (A–C) Decreased GFP-positive cell number in the triple transgenic animals (B) compared wild type littermates (A). Statistical analysis: 2-tailed unpaired *t*-test; $P < 0.0001$; +/+: $n = 6$; −/−: $n = 6$. Graph shows raw data points and means ± SEM. *n* indicates the number of mice per group. Scale bar indicates 100 µm (A,B); L1–6 marks cortical layers.

The Large Majority of Interneuron Subtypes in the Adult Cortex Are Not Affected by Postmitotic Loss of Cdh2

The adult Gad65-GFP data indicated that postmitotic Cdh2-loss had a long-term effect, so next, we wanted to know if it affected the various interneuron populations equally. In order to test this, we analyzed the adult somatosensory cortex using widely accepted markers of interneuron subpopulations (Wonders and Anderson 2006; Klausberger and Somogyi 2008; Gelman and Marín 2010). We failed to detect any changes in the number of Parvalbumin (PV)- or Reelin (*Reln*)-expressing interneurons between +/+ and −/− samples (Fig. 3A–C; (PV) +/+: $n = 6$, 155.7 ± 15.47; −/−: $n = 6$, 150.0 ± 7.332; $P = 0.8182$; Fig. 3D–F; (Reln) +/+: $n = 7$, 262.3 ± 13.59; −/−: $n = 7$, 237.4 ± 12.63; $P = 0.2086$). Similarly, *Vip*-expressing interneuron numbers were also not altered significantly (Fig. 3G–I; +/+: $n = 7$, 106 ± 4.602; −/−: $n = 7$, 106.6 ± 5.790; $P = 1$). Furthermore, the number of Npy-expressing cortical interneurons did also not change in *Cdh2*−/− cortical samples (Fig. 3J–L; +/+: $n = 7$, 185 ± 15.12; −/−: $n = 7$, 185.5 ± 17.55; $P = 1$). Finally, since Cck is also expressed in glutamatergic cells of the cortex, in order to mark the *Cck*-positive population we used the marker *Cnr1* that has an almost perfectly overlapping expression with Cck in all areas examined including the somatosensory cortex (Marsicano and Lutz 1999; Zeisel et al. 2015). These experiments, however, also did not reveal any alterations (Fig. 3M–O; +/+: $n = 8$, 128.7 ± 15.40; −/−: $n = 8$, 121.9 ± 10.81; $P = 0.9591$) in −/− animals.

Calretinin- and Somatostatin-Expressing Interneuron Numbers Decrease Significantly in the *Cdh2*−/− Somatosensory Cortex

In contrast to the cell types detailed above, a large drop (23.5%) was detectable in the number of *Calb2* (Calretinin)-positive interneurons (Fig. 4A–C; +/+: $n = 7$, 116 ± 3.542; −/−: $n = 7$, 88.8 ± 4.065; $P < 0.0001$) and this difference was also present at the protein level (Fig. 4G–I; +/+: $n = 6$, 69.98 ± 2.423; −/−: $n = 6$, 53.03 ± 2.123; $P < 0.0001$). Moreover, we found a smaller, but statistically significant (10%) decrease in the number of somatostatin-expressing cells of the adult somatosensory cortex of *Cdh2*−/− animals (Fig. 4D–F; +/+: $n = 11$, 212 ± 4.931; −/−: $n = 11$, 191.8 ± 4.62; $P = 0.0041$). Finally, we examined if there was an overlap between the missing *Sst* and *Calb2*-expressing populations. Indeed, immunohistochemistry revealed a large (36%) decrease in the number of *Sst*/*Calb2* double positive cells (Fig. 4G–HJ; +/+: $n = 6$, 11.62 ± 1.054; −/−: $n = 6$, 7.429 ± 0.55; $P = 0.0024$).

The results above clearly demonstrate that Cdh2 is required in a cell type-specific manner during postmitotic development of interneurons. Furthermore, the missing *Calb2*- and *Sst*-expressing cells did not undergo a fate-switch since we could not detect an increase in the cell numbers of the other interneuron populations.

The Gad65-GFP-Positive Precursors Are Arrested Prior to Radial Migration Into the Cortical Plate

Next, we wanted to know what happens between the embryonic migration delay (see Fig. 1) and the observed adult phenotype (see Fig. 2). In order to follow the fate of the interneuron precursors, we counted GFP-positive cells in the cortex of P8 triple transgenic mice (Fig. 5A–B,D; +/+: $N = 4$ 129.5 ± 4.632; −/−: $N = 4$ 96.62 ± 6.319; $P < 0.0001$), which revealed a significant decrease. Moreover, distribution analysis also demonstrated a shift in the number of GFP-positive neurons from the upper to the deepest 2 cortical bins indicating that the affected cells got arrested in the SVZ and layer 6/subplate layers (Fig. 5C; +/+ $n = 4$, −/− $n = 4$; Bin10: +/+: 19.33 ± 1.983, −/−: 47.92 ± 2.612, $P < 0.0001$).

The decrease in the number of adult cortical Gad65-GFP-expressing cells could be explained by several things, including a switch in their migratory routes to alternative target areas. Counting cells in the most likely alternative destinations such as the more lateral, supplemental somatosensory area cortex (Fig. 5E; +/+: $n = 4$, 375.8 ± 12.58; −/−: $n = 4$, 286.9 ± 12.53; $P < 0.0001$) and the striatum (Fig. 5F; +/+: $n = 4$, 42.82 ± 1.803; −/−: $n = 4$, 31.72 ± 2.200; $P = 0.0002$), however, revealed a similar decay in their numbers. This indicates that precursors originally destined to the dorsal cortex area did not get misrouted into these places. Moreover, these results also suggest that loss of Cdh2 from the subpallial postmitotic cells affects a much larger region, beyond the primary somatosensory cortex.

Developmental Delay Results in Increased Cell Death of the Cortical Interneuron Precursors in Postnatal Animals

With altered fate (Fig. 3) and migrational targeting (Fig. 5) discounted as possible explanations for the decreased interneuron numbers in the adult somatosensory cortex, we hypothesized

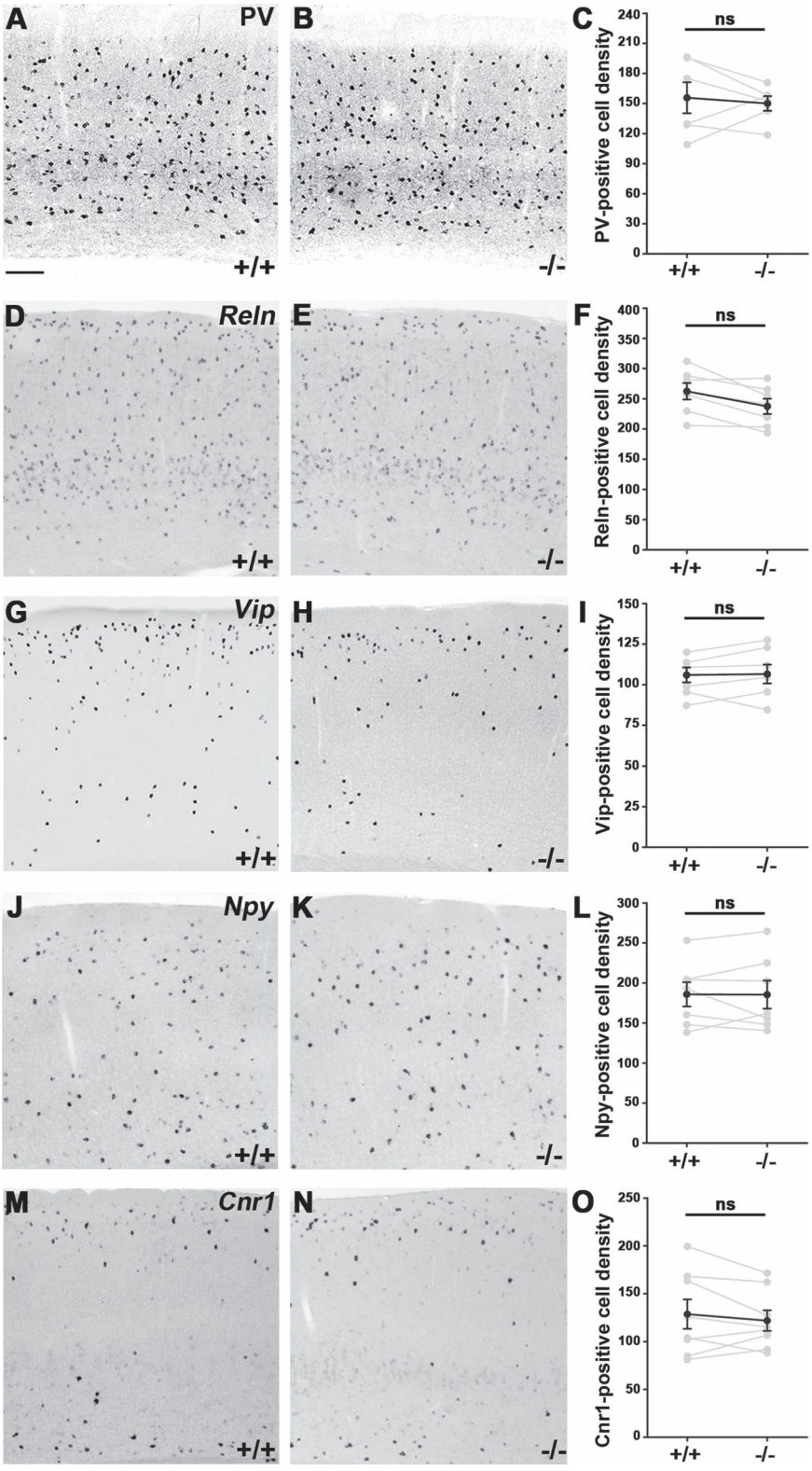

Figure 3. Quantitative comparison of various interneuron subtypes in the adult primer somatosensory cortex of +/+ and −/− animals. (A, B) Parvalbumin (PV) expression in the cortex of +/+ and −/− offsprings. (C) Statistical analysis: Mann–Whitney *U* test, $P = 0.8182$; +/+: $n = 6$; −/−: $n = 6$. (D, E) *Reelin (Reln)*-positive cells in the cortex. (F) Mann–Whitney *U* test, $P = 0.2086$; +/+: $n = 7$; −/−: $n = 7$. (G, H) *Vasoactive Intestinal Peptide (Vip)* expression. (I) Mann–Whitney *U* test, $P = 1$; +/+: $n = 7$; −/−: $n = 7$. (J, K) *Neuropeptide Y (Npy)*-positive cells in the somatosensory cortex. (L) Mann–Whitney *U* test, $P = 1$; +/+: $n = 7$; −/−: $n = 7$. (M–O) *Cannabinoid receptor 1 (Cnr1)*-positive cell numbers in littermates also show no significant differences between −/− and +/+ animals; Mann–Whitney *U* test, $P = 0.9591$; +/+: $n = 8$; −/−: $n = 8$. Statistical figures show mean values of sibling pairs (connected gray dots) and black connected dots represent means ± SEM. *n* indicates the number of mice per group. Scale bar shows 100 μm.

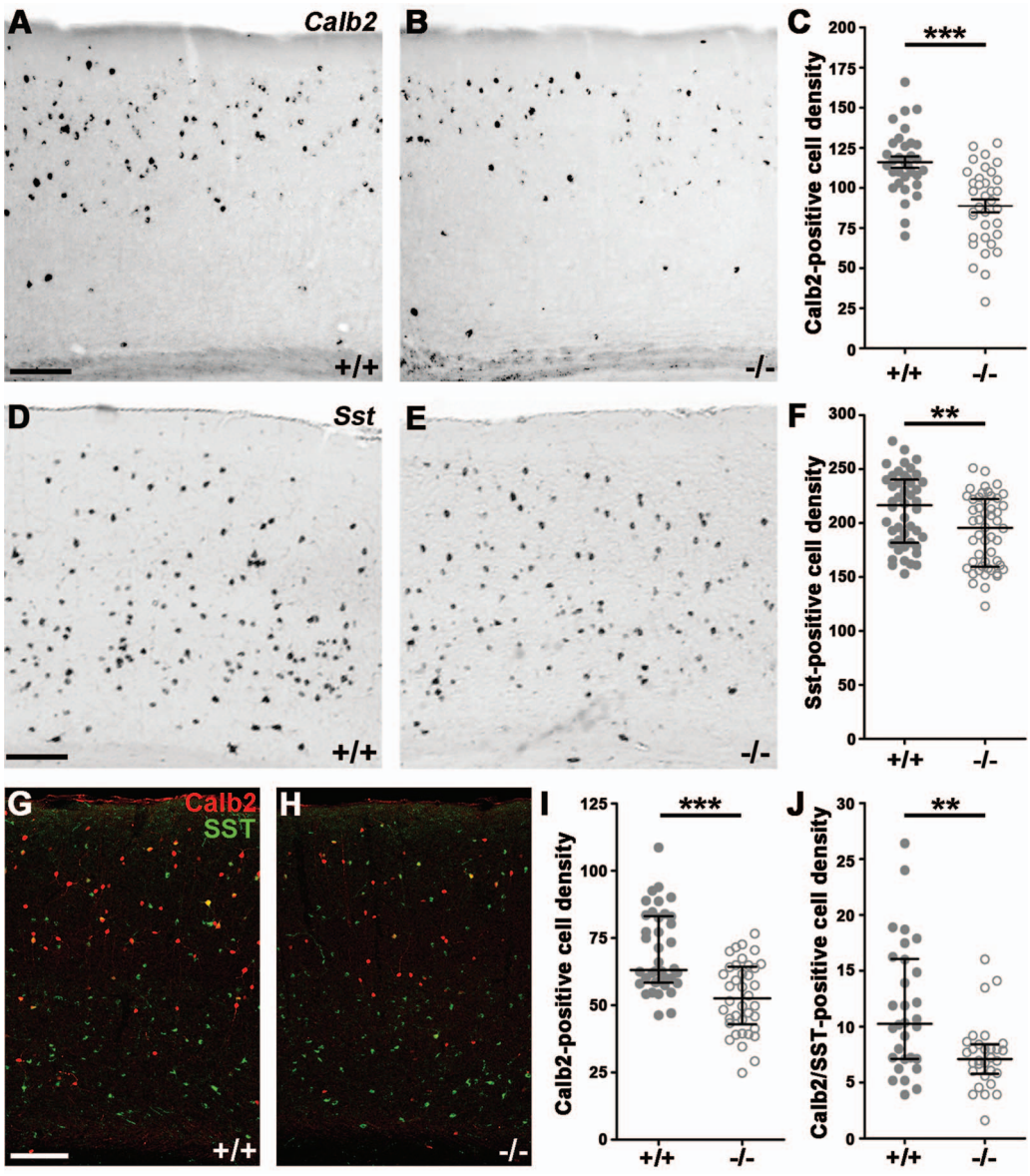

Figure 4. Elimination of Cdh2 from postmitotic precursors decreases calretinin and somatostatin interneuron cell numbers in the adult primer somatosensory cortex. (A, B) *Calretinin* (*Calb2*) in situ hybridization in +/+ (A) and −/− (B) animals. (C) Statistical analysis of Calb2-positive cell density shows significant difference between littermates. Two-tailed unpaired *t*-test, $P < 0.0001$; +/+: $n = 7$; −/−: $n = 7$; graph shows raw data points and means ± SEM. (D, E) *Somatostatin* (*Sst*) in situ hybridization in animal pairs. (F) Statistical analysis of Sst-positive cell density shows significant difference between +/+ and −/−. Mann–Whitney *U* test, $P = 0.0041$; +/+: $n = 11$; −/−: $n = 11$. Graph shows raw data points and medians ± interquartile range (IQR). (G, H) Sst and Calb2 double immunostaining. (I, J) Statistical analysis demonstrates a significant decrease in both Calb2-positive and Calb2/Sst double-positive cell density in −/− animals. Mann–Whitney *U* test, Calb2 $P < 0.0001$; Calb2/Sst $P = 0.0024$; +/+: $n = 6$; −/−: $n = 6$. Statistical figures show raw data points and medians ± interquartile range (IQR). *n* indicates the number of mice per group. Scale bars indicate 100 µm.

that the missing cells get eliminated at some point during development. In order to pinpoint the time of the proposed cell death, we carried out TUNEL assays at various time points of development. First, we analyzed cell death levels in the E14 ganglionic eminence (Fig. 6A,B; +/+: $n = 3$, 23.56 ± 1.988; −/−: $n = 3$, 22.09 ± 1.289; $P = 0.7535$) as well as in the future striatal area (Fig. 6A,C; +/+: $n = 3$, 5.194 ± 0.519, −/−: $n = 3$, 5.903 ± 0.622; $P = 0.5429$). This experiment however, revealed no differences between +/+ and −/− embryos, excluding the possibility of increased early cell death being responsible for lower interneuron numbers in the adult cortex. In contrast, the number of TUNEL-positive cells was significantly increased in the dorsolateral cortex of P8 littermates (Fig. 6D–F; +/+: $n = 5$, 51.74 ± 2.336; −/−: $n = 5$, 80.09 ± 2.393; $P < 0.0001$). Moreover, distribution analysis revealed that this elevation is restricted to the highest and lowest bins of the cortex largely corresponding to the marginal and SVZs, respectively (Fig. 6G; +/+ $n = 5$, −/− $n = 5$; Bin1: +/+: 19.53 ± 2.318, −/−: 8.235 ± 0.8303, $P < 0.0001$; Bin10: +/+: 35.17 ± 2.756, −/−: 56.12 ± 2.155, $P < 0.0001$). Coincidentally, these are the main areas of tangential migration and the SVZ is where the developmentally arrested cells accumulated (Fig. 5A–C). When taken together, our data strongly suggest that delayed interneuron precursors, which do not enter the cortical plate by early postnatal stages get eliminated.

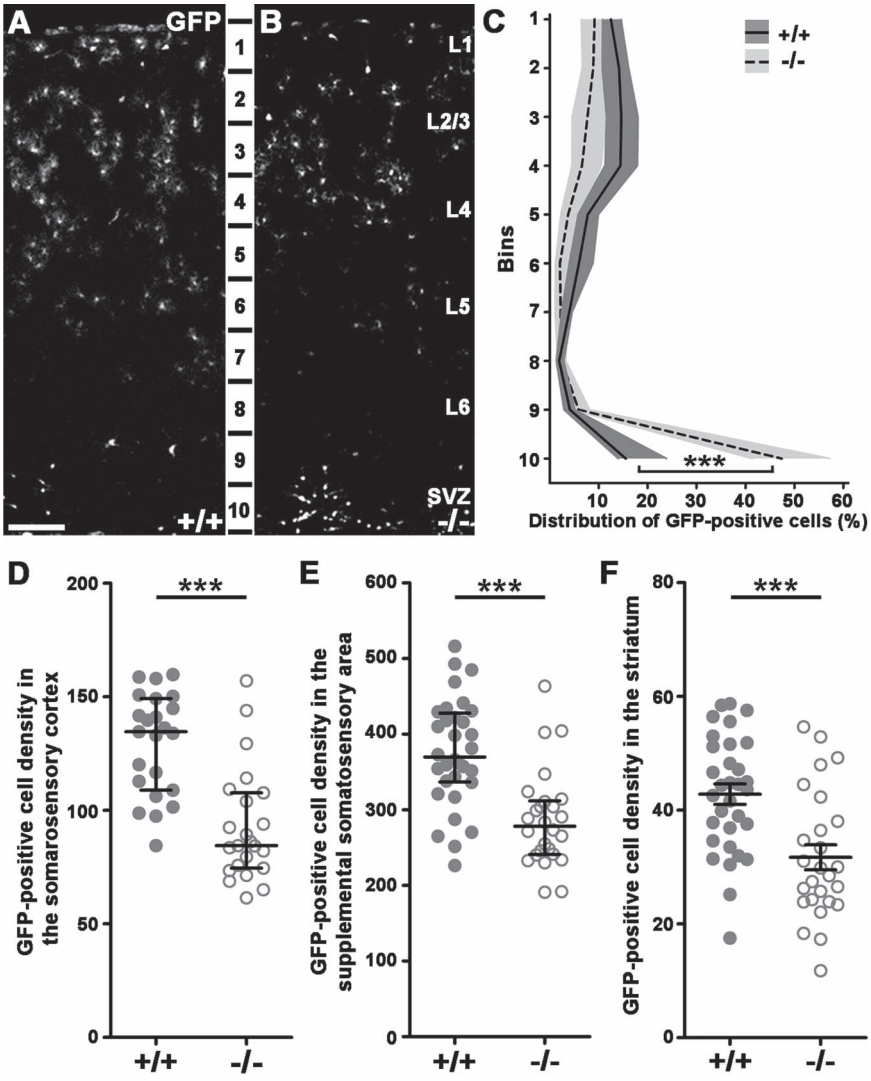

Figure 5. Arrested cortical migration and decreased GAD65-GFP-positive interneuron density in P8 triple transgenic brains. (A–B) GFP-positive interneuron distribution in P8 littermates. (C) Distribution analysis in 10 equal cortical bins illustrates cell density changes in the −/− animals. Statistical analysis compared siblings in every bin: Bin1: Mann–Whitney *U* test, $P = 0.0023$; Bin2: 2-tailed unpaired *t*-test, $P < 0.0001$; Bin3: 2-tailed unpaired *t*-test, $P = 0.0007$; Bin4: 2-tailed unpaired *t*-test, $P < 0.0001$; Bin5: 2-tailed unpaired *t*-test, $P < 0.0001$; Bin6: Mann–Whitney *U* test, $P < 0.0001$; Bin7: 2-tailed unpaired *t*-test, $P = 0.0375$; Bin8: Mann–Whitney *U* test, $P = 0.4654$; Bin9: Mann–Whitney *U* test, $P = 0.0024$; Bin10: Mann–Whitney *U* test, $P < 0.0001$; +/+: $n = 4$; −/− $n = 4$. Graph shows median ± interquartile range (IQR). (D–F) Statistical analysis of GFP-positive cell density in different brain regions. Significant statistical difference occurs between +/+ and −/− animals in the somatosensory cortex (D; +/+: $n = 4$; −/− $n = 4$; Mann–Whitney *U* test; $P < 0.0001$), supplemental somatosensory area (E; +/+: $n = 4$; −/− $n = 4$; Mann–Whitney *U* test; $P < 0.0001$), as well as in the striatum (F; +/+: $n = 4$; −/− $n = 4$; 2-tailed unpaired *t*-test; $P = 0.0002$). Statistical figures show raw data points and medians ± interquartile range (IQR; D, E) or means ± SEM (F). *n* indicates the number of mice per group. Scale bars indicate 100 µm (A–B); L: layer.

Discussion

The Role of Cdh2 in Cortical Neurogenesis

Cell adhesion and migration are heavily interdependent during both normal and pathological development of the pallial neocortex, and Cdh2 has been established as one of the main adhesion molecules involved in these processes (Kadowaki et al. 2007; Rousso et al. 2012). Cdh2 homodimer-based adherent junctions found here have a dual role: they connect radial glia cells thereby preventing mobility of dividing precursors and control their proliferation (Zhang et al. 2010, 2013; Jossin and Cooper 2011; Gil-Sanz et al. 2014). In addition, loss of Cdh2 from radial glia cells also damages the glial scaffold and severely disrupts radial migration of excitatory neuron precursors, which in turn prevents proper cortical lamination (Kadowaki et al. 2007; Franco et al. 2011; Gil-Sanz et al. 2013). Similarly, it has been reported (Luccardini et al. 2013) that lack of Cdh2 in the VZ of the ganglionic eminences also results in proliferation defects and failure of interneuron precursor migration. Ganglionic eminence-derived neuroblasts from *Cdh2*−/− animals lose their polarity leading to severe disruption of directionality and decreased speed of migration (Luccardini et al. 2013) due to defective synchronization of centrosomal and nuclear movements (Luccardini et al. 2015). In summary, loss of Cdh2 in the proliferating interneuron progenitors resembles closely to that of found in loss-of-function models for radial glia progenitors in rodents (Kadowaki et al. 2007) and for neuroepithelial cells in lower vertebrates (Gänzler-Odenthal and Redies 1998; Lele et al. 2002).

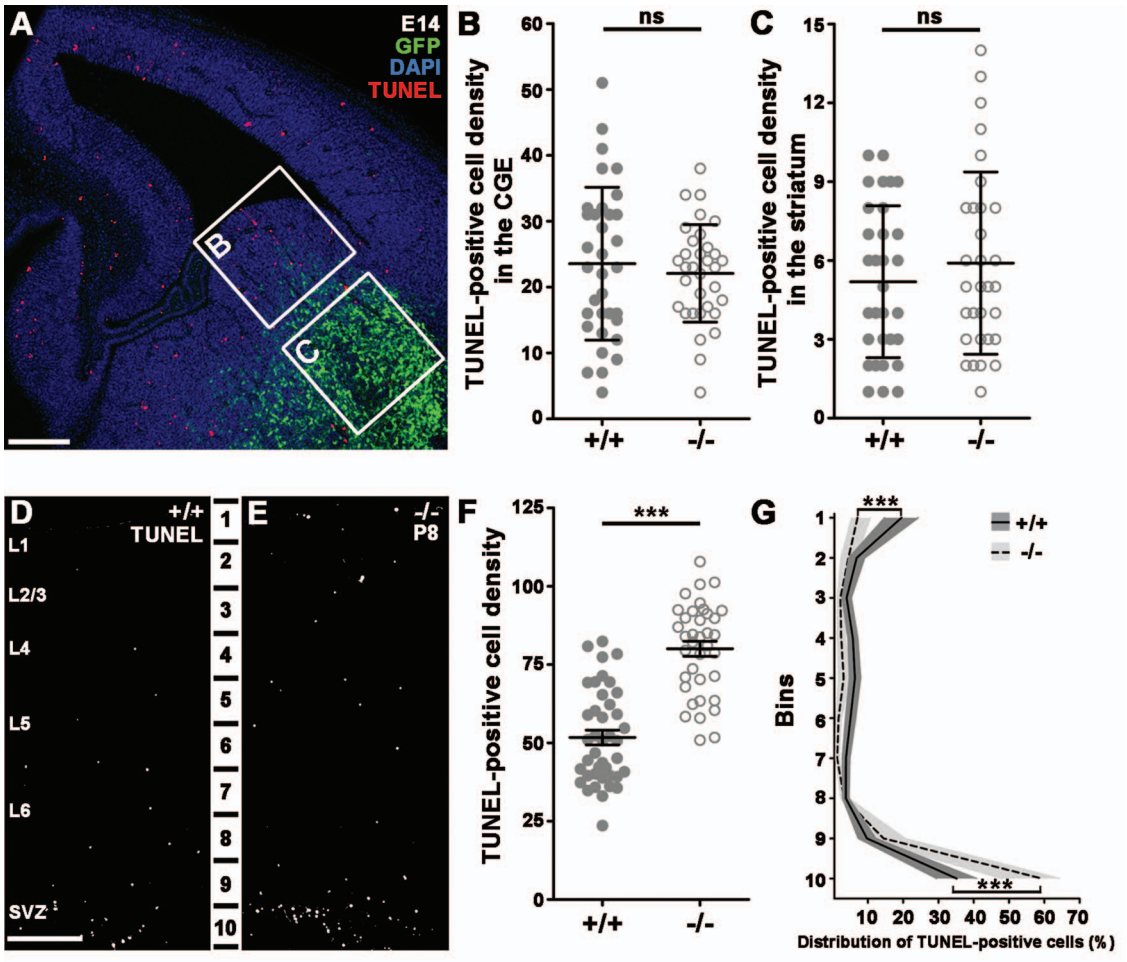

Figure 6. Increased cell death in the somatosensory cortex of postnatal −/− animals. (A) TUNEL-stained E14 brain slice shows example quadrates for statistical analysis from CGE (B) and developing striatum (C). (B–C) Statistical analysis of TUNEL-positive cell density from distinct areas: CGE; Mann–Whitney *U* test, $P = 0.7535$; striatum: Mann–Whitney *U* test, $P = 0.5429$; +/+: $n = 3$; −/− $n = 3$. Graphs show raw data points and medians ± interquartile range (IQR). (D–E) P8 TUNEL-stained brain slices from +/+ (D) and −/− (E) animals. (F) Statistical analysis of TUNEL-positive cell density in the somatosensory cortex shows significant difference between littermates. +/+: $n = 5$; −/− $n = 5$; 2-tailed unpaired *t*-test; $P < 0.0001$, graph shows raw data points and means ± SEM. (G) Distribution analysis of TUNEL-positive cells in 10 equal bins. Bin1: Mann–Whitney *U* test, $P < 0.0001$; Bin2: Mann–Whitney *U* test, $P = 0.4041$; Bin3: Mann–Whitney *U* test, $P = 0.2744$; Bin4: Mann–Whitney *U* test, $P = 0.0004$; Bin5: Mann–Whitney *U* test, $P = 0.0045$; Bin6: Mann–Whitney *U* test, $P < 0.0001$; Bin7: Mann–Whitney *U* test, $P = 0.0003$; Bin8: Mann–Whitney *U* test, $P = 1$; Bin9: Mann–Whitney *U* test, $P = 0.1$; 2-tailed unpaired *t*-test, $P < 0.0001$; +/+: $n = 5$; −/− $n = 5$. Graph shows median ± interquartile range (IQR). *n* indicates the number of mice per group. Scale bars indicate 100 µm (A), 50 µm (D–E); L: layer.

Here, we complete this picture by establishing the necessity of Cdh2 during the postmitotic phase of interneuron development. We demonstrate that loss of Cdh2 in postmitotic neuroblasts results in decreased numbers of Gad65-GFP-expressing interneurons in the adult cortex. Our data exclude proliferation, early apoptosis, alternative migration destinations, and cell-fate alteration as potential sources for the decreased number of interneurons in the adult somatosensory cortex. Finally, we show that this defect can be traced back to an early prenatal migration delay followed by postnatal elimination of mislocalized precursors.

The Cell-Type Specificity of N-cadherin Removal in Postmitotic Interneuron Development

Our experiments were also the first to examine the long-term effect of N-cadherin removal in migrating neuroblasts. Surprisingly, we observed a cell-type-specific need for Cdh2 during migration of *Calb2*- and *Sst*-expressing interneuron precursors. Similar subtype-selectivity was not investigated for glutamatergic cells in pallial Cdh2 loss-of-function models, although analyzing subtypes of glutamatergic cells would be technically more challenging and invariably require single cell RNAseq and/or electrophysiological techniques (Tasic et al. 2016).

Cortical interneuron populations have been studied extensively using morphological, molecular, and physiological markers (Tremblay et al. 2016; Habib et al. 2017; Lim et al. 2018). As a general rule, Sst-positive interneurons are mainly produced in the MGE while Calb2-positive cells are mostly born in the CGE. There is a common population of interneurons born at the dorsal MGE however, which express both Sst and Calb2 (Xu et al. 2006; Fogarty et al. 2007; Wonders et al. 2008; Sousa et al. 2009) and there is also a report of Sst-expressing cell population originating from the CGE (Mi et al. 2018). Recently, several studies have carried out detailed morphological and physiological characterization of the Sst-positive interneuron population of the

cortex (Ma 2006; He et al. 2016; Muñoz et al. 2017; Nigro et al. 2018). Based on their and our results, it seems likely that at least some of the cells eliminated by the loss of Cdh2 are Martinotti cell precursors. It is important to note, however, that not all Calb2/Sst double positive cells are eliminated from the brain of *Cdh2−/−* animals, indicating a further diversity within this population despite earlier claims that described a single Sst/Calb2 population in the mouse cortex (Zeisel et al. 2015). Our observation, however, has been supported by a recent large-scale single-cell RNAseq research study, which indeed reported the presence of 2 Sst-Calb2 populations in the adult mouse cortex (Tasic et al. 2018). Finally, it is important to point out that the decrease in Calb2-positive cell numbers exceeds significantly those found in the Sst-positive population. This indicates that there is also a Sst-negative/Calb-positive cell population missing from the *Cdh−/−* cortex. This population is likely lost from the Reelin-positive cells, since we detected absolutely no changes in the Vip-positive cell population. In contrast, Reelin cell density displayed a decreasing tendency (approx. 10% in −/−), which was stastistically not significant only due to the large number of Reelin-positive cells.

The Molecular Background of the Differential Cdh2-Dependency of Interneuron Precursors

Naturally, the question emerges, what is behind the cell type-specific need for Cdh2? The first and most obvious answer is genetic redundancy and clearly, multiple classic cadherins, particularly from the type II family, are present in the migration path of interneuron precursors, which could complement for the loss of Cdh2 (Lefkovics et al. 2012). To prove this, however, multiple knockout experiments would be necessary, which might be very challenging but considering recent advancements in loss-of-function gene technology (Crisp/Cas9 and Zn2 + −finger nucleases), not entirely impossible.

Alternatively, differential regulation of Cdh2 levels in various interneuron precursor populations can also cause some of them to be more or less dependent on Cdh2. Earlier, extensive studies have revealed a complex network of homeobox transcription factors that determine interneuron fate already in the subpallium (Wonders and Anderson 2006; Gelman and Marín 2010; Kessaris et al. 2014). Notably, there is a transcription factor, Nkx6.2, which is expressed exclusively in the dorsal MGE where Calb2/Sst-positive cells are born (Fogarty et al. 2007; Wonders et al. 2008; Sousa et al. 2009). More importantly, lineage analysis of Nkx6.2-Cre; Rosa26R-GFP PAC double transgenic mice indicated that Calb2/Sst-positive neurons, which are also heavily affected by Cdh2-loss in our experiments, strongly co-express Nkx6.2-driven GFP (Fogarty et al. 2007). Furthermore, similarly to what we found in *Cdh2−/−* mice, there is a partial loss of the Sst/Calb2 double-positive cell population in *Nkx6.2−/−* animals (Sousa et al. 2009). Considering all these experiments, it would be extremely interesting to see whether Nkx6.2 directly or indirectly regulates *Cdh2* expression.

Finally, the answer to the question of cell-type specificity might come from the fact that different interneuron groups are born at specific times and places in the subpallium (Butt et al. 2007; Nakajima 2007; Marín 2013). Therefore, it seems like a distinct possibility, that there is a strict time window when interneuron precursors can enter into the cortical plate. After this, structural changes in the subplate or simply the presence of the quickly increasing number of thalamocortical axons prevents the entry (Hoerder-Suabedissen and Molnár 2015). Since CGE-derived (hence the majority of Calb2-expressing) interneurons are among the last ones to differentiate (Nery et al. 2002; Xu 2004; Fogarty et al. 2007; Miyoshi et al. 2007; Laclef and Métin 2018), it is possible that even a slight delay can make the precursors miss this time window and get arrested below the subplate. Consequently, these cells are not able to incorporate into the cortical circuitry, which is essential for the extrinsic neuronal activity-based support of their proper development (De Marco García et al. 2011) and survival (Priya et al. 2018; Wong et al. 2018).

In summary, loss of Cdh2 function in postmitotic neuroblasts has revealed a cell-type specific need for this protein during tangential migration and survival of Calb2- and Sst-positive interneuron precursors. Defective migration of interneurons is considered widely to be a major factor in several neurodevelopmental disorders, like epilepsy, autism spectrum disorder, and schizophrenia (Levitt et al. 2004; Rubenstein 2011; Marín 2012; Lewis 2014). Specifically, decreased number of calretinin-expressing interneurons has recently been linked to autism (Adorjan et al. 2017) and amyotrophic lateral sclerosis (Clark et al. 2017). As progenitor transplantation is becoming more and more feasible as a potential treatment for these diseases (Southwell et al. 2014; Tyson and Anderson 2014), shedding light on the necessary molecular elements required for the survival of individual interneuron cell types will be crucial.

Funding

Hungarian Scientific Research Fund (OTKA, F 68177 to Z.L.); the European Research Council Grant (243153 to I.K.); the National Research, Development and Innovation Office, Hungary (VKSZ_14-1-2O15-0155 to I.K.); the Hungarian Brain Research Program (2017-1.2.1-NKP-2017-00002 to I.K.); the Hungarian Scientific Research Fund (OTKA, K 116915 to I.K.); the Momentum Program of the Hungarian Academy of Sciences (LP2013-54/2013 to I.K.); the Wellcome Trust International Senior Research Fellowship (090946/Z/09/Z to I.K.); Semmelweis University Predoctoral Grant (EFOP-3.6.3-VEKOP-16-2017-00009 to Z.I.L.); the Swiss Contribution grant (SH/7/2/18 to I.K.).

Notes

We are grateful to J.L.R. Rubenstein for providing us the dlx5/6-Cre mouse line; we thank Medical Genetics Unit of IEM HAS for help in keeping and breeding our mouse lines. We also thank the NIKON Microscopy Center based in IEM-HAS for providing help with image acquisition and analysis. *Conflict of Interest*: None declared.

References

Adorjan I, Ahmed B, Feher V, Torso M, Krug K, Esiri M, Chance SA, Szele FG. 2017. Calretinin interneuron density in the caudate nucleus is lower in autism spectrum disorder. *Brain*. 140:2028–2040.

Ang ESBC, Haydar TF, Gluncic V, Rakic P. 2003. Four-dimensional migratory coordinates of GABAergic interneurons in the developing mouse cortex. *J Neurosci*. 23:5805–5815.

Ayala R, Shu T, Tsai L-H. 2007. Trekking across the brain: the journey of neuronal migration. *Cell*. 128:29–43.

Butt SJB, Cobos I, Golden J, Kessaris N, Pachnis V, Anderson S. 2007. Transcriptional regulation of cortical interneuron development. *J Neurosci*. 27:11847–11850.

Bystron I, Blakemore C, Rakic P. 2008. Development of the human cerebral cortex: Boulder Committee revisited. *Nat Rev Neurosci*. 9:110–122.

Clark RM, Blizzard CA, Young KM, King AE, Dickson TC. 2017. Calretinin and neuropeptide y interneurons are differentially altered in the motor cortex of the SOD1 G93A mouse model of ALS. *Sci Rep*. 7:1–13.

De Marco García NV, Karayannis T, Fishell G. 2011. Neuronal activity is required for the development of specific cortical interneuron subtypes. *Nature*. 472:351–355.

Fogarty M, Grist M, Gelman D, Marin O, Pachnis V, Kessaris N. 2007. Spatial genetic patterning of the embryonic neuroepithelium generates GABAergic interneuron diversity in the adult cortex. *J Neurosci*. 27:10935–10946.

Franco SJ, Martinez-Garay I, Gil-Sanz C, Harkins-Perry SR, Müller U. 2011. Reelin regulates cadherin function via Dab1/Rap1 to control neuronal migration and lamination in the neocortex. *Neuron*. 69:482–497.

Gänzler-Odenthal SII, Redies C. 1998. Blocking N-cadherin function disrupts the epithelial structure of differentiating neural tissue in the embryonic chicken brain. *J Neurosci*. 18:5415–5425.

Gelman DM, Marín O. 2010. Generation of interneuron diversity in the mouse cerebral cortex. *Eur J Neurosci*. 31:2136–2141.

Ghanem N. 2003. Regulatory roles of conserved intergenic domains in vertebrate Dlx bigene clusters. *Genome Res*. 13:533–543.

Ghanem N, Yu M, Long J, Hatch G, Rubenstein JLR, Ekker M. 2007. Distinct cis-regulatory elements from the Dlx1/Dlx2 locus mark different progenitor cell populations in the ganglionic eminences and different subtypes of adult cortical interneurons. *J Neurosci*. 27:5012–5022.

Ghanem N, Yu M, Poitras L, Rubenstein JLR, Ekker M. 2008. Characterization of a distinct subpopulation of striatal projection neurons expressing the Dlx genes in the basal ganglia through the activity of the I56ii enhancer. *Dev Biol*. 322:415–424.

Gil-Sanz C, Franco SJ, Martinez-Garay I, Espinosa A, Harkins-Perry S, Müller U. 2013. Cajal–Retzius cells instruct neuronal migration by coincidence signaling between secreted and contact-dependent guidance cues. *Neuron*. 79:461–477.

Gil-Sanz C, Landeira B, Ramos C, Costa MR, Muller U. 2014. Proliferative defects and formation of a double cortex in mice lacking Mltt4 and Cdh2 in the dorsal telencephalon. *J Neurosci*. 34:10475–10487.

Habib N, Avraham-Davidi I, Basu A, Burks T, Shekhar K, Hofree M, Choudhury SR, Aguet F, Gelfand E, Ardlie K *et al*. 2017. Massively parallel single-nucleus RNA-seq with DroNc-seq. *Nat Methods*. 14:955–958.

He M, Tucciarone J, Lee S, Nigro MJ, Kim Y, Levine JM, Kelly SM, Krugikov I, Wu P, Chen Y *et al*. 2016. Strategies and tools for combinatorial targeting of GABAergic neurons in mouse cerebral cortex. *Neuron*. 91:1228–1243.

Hirano S, Takeichi M. 2012. Cadherins in brain morphogenesis and wiring. *Physiol Rev*. 92:597–634.

Hoerder-Suabedissen A, Molnár Z. 2015. Development, evolution and pathology of neocortical subplate neurons. *Nat Rev Neurosci*. 16:133–146.

Hulpiau P, van Roy F. 2009. Molecular evolution of the cadherin superfamily. *Int J Biochem Cell Biol*. 41:349–369.

Jossin Y, Cooper JA. 2011. Reelin, Rap1 and N-cadherin orient the migration of multipolar neurons in the developing neocortex. *Nat Neurosci*. 14:697–703.

Kadowaki M, Nakamura S, Machon O, Krauss S, Radice GL, Takeichi M. 2007. N-cadherin mediates cortical organization in the mouse brain. *Dev Biol*. 304:22–33.

Kawauchi T, Sekine K, Shikanai M, Chihama K, Tomita K, Kubo KI, Nakajima K, Nabeshima YI, Hoshino M. 2010. Rab GTPases-dependent endocytic pathways regulate neuronal migration and maturation through N-cadherin trafficking. *Neuron*. 67:588–602.

Kessaris N, Magno L, Rubin AN, Oliveira MG. 2014. Genetic programs controlling cortical interneuron fate. *Curr Opin Neurobiol*. 26:79–87.

Klausberger T, Somogyi P. 2008. Neuronal diversity and temporal dynamics: the unity of hippocampal circuit operations. *Science (80-)*. 321:53–57.

Kriegstein AR, Noctor SC. 2004. Patterns of neuronal migration in the embryonic cortex. *Trends Neurosci*. 27:392–399.

Laclef C, Métin C. 2018. Conserved rules in embryonic development of cortical interneurons. *Semin Cell Dev Biol*. 76:86–100.

Lefkovics K, Mayer M, Bercsényi K, Szabó G, Lele Z. 2012. Comparative analysis of type II classic cadherin mRNA distribution patterns in the developing and adult mouse somatosensory cortex and hippocampus suggests significant functional redundancy. *J Comp Neurol*. 520:1387–1405.

Lele Z, Folchert A, Concha M, Rauch G-J, Geisler R, Rosa F, Wilson SW, Hammerschmidt M, Bally-Cuif L. 2002. Parachute/N-cadherin is required for morphogenesis and maintained integrity of the zebrafish neural tube. *Development*. 129:3281–3294.

Letinic K, Rakic P. 2001. Telencephalic origin of human thalamic GABAergic neurons. *Nat Neurosci*. 4:931–936.

Levitt P, Eagleson KL, Powell EM. 2004. Regulation of neocortical interneuron development and the implications for neurodevelopmental disorders. *Trends Neurosci*. 27:400–406.

Lewis DA. 2014. Inhibitory neurons in human cortical circuits: substrate for cognitive dysfunction in schizophrenia. *Curr Opin Neurobiol*. 26:22–26.

Lim L, Mi D, Llorca A, Marín O. 2018. Development and functional diversification of cortical interneurons. *Neuron*. .

Linford A, Yoshimura S, Bastos RN, Langemeyer L, Gerondopoulos A, Rigden DJ, Barr FA. 2012. Rab14 and its exchange factor FAM116 link endocytic recycling and adherens junction stability in migrating cells. *Dev Cell*. 22:952–966.

López-Bendito G, Sturgess K, Erdélyi F, Szabó G, Molnár Z, Paulsen O. 2004. Preferential origin and layer destination of GAD65-GFP cortical interneurons. *Cereb Cortex*. 14:1122–1133.

Luccardini C, Hennekinne L, Viou L, Yanagida M, Murakami F, Kessaris N, Ma X, Adelstein RS, Mege R-M, Metin C. 2013. N-cadherin sustains motility and polarity of future cortical interneurons during tangential migration. *J Neurosci*. 33:18149–18160.

Luccardini C, Leclech C, Viou L, Rio J-P, Métin C. 2015. Cortical interneurons migrating on a pure substrate of N-cadherin exhibit fast synchronous centrosomal and nuclear movements and reduced ciliogenesis. *Front Cell Neurosci*. 9:1–15.

Ma Y. 2006. Distinct subtypes of somatostatin-containing neocortical interneurons revealed in transgenic mice. *J Neurosci*. 26:5069–5082.

Marín O. 2012. Interneuron dysfunction in psychiatric disorders. *Nat Rev Neurosci*. 13:107–120.

Marín O. 2013. Cellular and molecular mechanisms controlling the migration of neocortical interneurons. *Eur J Neurosci*. 38:2019–2029.

Marín O, Rubenstein JLR. 2003. Cell migration in the forebrain. *Annu Rev Neurosci*. 26:441–483.

Marsicano G, Lutz B. 1999. Expression of the cannabinoid receptor CB1 in distinct neuronal subpopulations in the adult mouse forebrain. *Eur J Neurosci*. 11:4213–4225.

Mayer C, Hafemeister C, Bandler RC, Machold R, Batista Brito R, Jaglin X, Allaway K, Butler A, Fishell G, Satija R. 2018. Developmental diversification of cortical inhibitory interneurons. *Nature*. 555:457–462.

Mayer M, Bercsényi K, Géczi K, Szabó G, Lele Z. 2010. Expression of two type II cadherins, Cdh12 and Cdh22 in the developing and adult mouse brain. *Gene Expr Patterns*. 10:351–360.

Metin C, Vallee RB, Rakic P, Bhide PG. 2008. Modes and mishaps of neuronal migration in the mammalian brain. *J Neurosci*. 28:11746–11752.

Mi D, Li Z, Lim L, Li M, Moissidis M, Yang Y, Gao T, Hu TX, Pratt T, Price DJ *et al*. 2018. Early emergence of cortical interneuron diversity in the mouse embryo. *Science (80-)*. 360:81–85.

Miyoshi G, Butt SJB, Takebayashi H, Fishell G. 2007. Physiologically distinct temporal cohorts of cortical interneurons arise from telencephalic olig2-expressing precursors. *J Neurosci*. 27:7786–7798.

Monory K, Nave K-A, Kelsch W, Dodt H-U, During M, Lutz B, Wölfel B, Long J, Klugmann M *et al*. 2006. The endocannabinoid system controls key epileptogenic circuits in the hippocampus. *Neuron*. 51:455–466.

Muñoz W, Tremblay R, Levenstein D, Rudy B. 2017. Layer-specific modulation of neocortical dendritic inhibition during active wakefulness. *Science (80-)*. 355:954–959.

Nakajima K. 2007. Control of tangential/non-radial migration of neurons in the developing cerebral cortex. *Neurochem Int*. 51:121–131.

Nery S, Fishell G, Corbin JG. 2002. The caudal ganglionic eminence is a source of distinct cortical and subcortical cell populations. *Nat Neurosci*. 5:1279–1287.

Nigro MJ, Hashikawa-Yamasaki Y, Rudy B. 2018. Diversity and connectivity of layer 5 somatostatin-expressing interneurons in the mouse barrel cortex. *J Neurosci*. 38:1622–1633.

Parnavelas JG. 2000. The origin and migration of cortical neurones: new vistas. *Trends Neurosci*. 23:126–131.

Priya R, Paredes MF, Karayannis T, Yusuf N, Liu X, Jaglin X, Graef I, Alvarez-Buylla A, Fishell G. 2018. Activity regulates cell death within cortical interneurons through a calcineurin-dependent mechanism. *Cell Rep*. 22:1695–1709.

Radonjić NV, Ayoub AE, Memi F, Yu X, Maroof A, Jakovcevski I, Anderson SA, Rakic P, Zecevic N. 2014. Diversity of cortical interneurons in primates: the role of the dorsal proliferative niche. *Cell Rep*. 9:2139–2151.

Redies C, Ast M, Nakagawa S, Takeichi M, Martínez-De-La-Torre M, Puelles L. 2000. Morphologic fate of diencephalic prosomeres and their subdivisions revealed by mapping cadherin expression. *J Comp Neurol*. 421:481–514.

Rousso DL, Pearson CA, Gaber ZB, Miquelajauregui A, Li S, Portera-Cailliau C, Morrisey EE, Novitch BG. 2012. Foxp-mediated suppression of N-cadherin regulates neuroepithelial character and progenitor maintenance in the CNS. *Neuron*. 74:314–330.

Rubenstein JLR. 2011. Annual research review: development of the cerebral cortex: implications for neurodevelopmental disorders. *J Child Psychol Psychiatry Allied Discip*. 52:339–355.

Sousa VH, Miyoshi G, Hjerling-Leffler J, Karayannis T, Fishell G. 2009. Characterization of Nkx6-2-derived neocortical interneuron lineages. *Cereb Cortex*. 19:1–10.

Southwell DG, Nicholas CR, Basbaum AI, Stryker MP, Kriegstein AR, Rubenstein JL, Alvarez-Buylla A. 2014. Interneurons from embryonic development to cell-based therapy. *Science (80-)*. 344:1240622–1240622.

Takeichi M, Abe K. 2005. Synaptic contact dynamics controlled by cadherin and catenins. *Trends Cell Biol*. 15:216–221.

Tasic B, Menon V, Nguyen TN, Kim TK, Jarsky T, Yao Z, Levi B, Gray LT, Sorensen SA, Dolbeare T *et al*. 2016. Adult mouse cortical cell taxonomy revealed by single cell transcriptomics. *Nat Neurosci*. 19:335–346.

Tasic B, Yao Z, Graybuck LT, Smith KA, Nguyen TN, Bertagnolli D, Goldy J, Garren E, Economo MN, Viswanathan S *et al*. 2018. Shared and distinct transcriptomic cell types across neocortical areas. *Nature*. 20.

Tremblay R, Lee S, Rudy B. 2016. GABAergic interneurons in the neocortex: from cellular properties to circuits. *Neuron*. 91:260–292.

Tyson JA, Anderson SA. 2014. GABAergic interneuron transplants to study development and treat disease. *Trends Neurosci*. 37:169–177.

Valiente M, Marín O. 2010. Neuronal migration mechanisms in development and disease. *Curr Opin Neurobiol*. 20:68–78.

Wonders CP, Anderson SA. 2006. The origin and specification of cortical interneurons. *Nat Rev Neurosci*. 7:687–696.

Wonders CP, Taylor L, Welagen J, Mbata IC, Xiang JZ, Anderson SA. 2008. A spatial bias for the origins of interneuron subgroups within the medial ganglionic eminence. *Dev Biol*. 314:127–136.

Wong FK, Bercsenyi K, Sreenivasan V, Portalés A, Fernández-Otero M, Marín O. 2018. Pyramidal cell regulation of interneuron survival sculpts cortical networks. *Nature*. 557:668–673.

Xu Q. 2004. Origins of cortical interneuron subtypes. *J Neurosci*. 24:2612–2622.

Xu X, Roby KD, Callaway EM. 2006. Mouse cortical inhibitory neuron type that coexpresses somatostatin and calretinin. *J Comp Neurol*. 499:144–160.

Zeisel A, Munoz-Manchado AB, Codeluppi S, Lonnerberg P, La Manno G, Jureus A, Marques S, Munguba H, He L, Betsholtz C *et al*. 2015. Cell types in the mouse cortex and hippocampus revealed by single-cell RNA-seq. *Science (80-)*. 347:1138–1142.

Zhang J, Shemezis JR, McQuinn ER, Wang J, Sverdlov M, Chenn A. 2013. AKT activation by N-cadherin regulates beta-catenin signaling and neuronal differentiation during cortical development. *Neural Dev*. 8:7.

Zhang J, Woodhead GJ, Swaminathan SK, Noles SR, McQuinn ER, Pisarek AJ, Stocker AM, Mutch CA, Funatsu N, Chenn A. 2010. Cortical neural precursors inhibit their own differentiation via N-cadherin maintenance of β-catenin signaling. *Dev Cell*. 18:472–479.